Supporting Information

Zn(II)/Cd(II)-based metal-organic frameworks: crystal structures, Ln(III)-functionalized luminescence and chemical sensing of dichloroaniline as pesticide biomarker

Xiang-Long Qu[a] and Bing Yan[a,b]*

[a] Shanghai Key Lab of Chemical Assessment and Sustainability, School of Chemical Science and Engineering, Tongji University, Shanghai 200092, China

[b] School of Materials Science and Engineering, Liaocheng University, Liaocheng 252059, China

Chemical stability experiments: the crystal samples of **1-4** (50 mg) were placed in round-bottomed flasks containing several common solvents including cyclohexane, benzene, ethyl acetate, acetone, ethanol, methanol, N, N'- dimethylformamide (DMF), water for two days' storage before the samples were subjected to PXRD measurements for chemical stabilities studies.

Sensitivity experiments in reconstituted urine: as for the sensitivity studies of sensing 3, 4-DCA and 3,5-DCA in reconstituted urine samples, 3 mg of Tb(III)@**4** powder was simply immersed into the 3 mL DMF/urine solutions (v/v, 10/1) treated by ultrasonication for approximately 10 min. The real-time luminescence spectra of the Tb(III)@**4** suspensions were then measured based on multiple addition of a certain concentration of dichloroanilines DMF solution (50 μL).

Concentration-dependent lifetime experiments: 3 mg of Tb(III)@**4** powder was simply immersed into the 3 mL DMF solutions treated by ultrasonication for approximately 10 min. The real-time lifetimes of the Tb(III)@**4** towards 3, 4-DCA and 3, 5-DCA were measured based on multiple addition of a certain concentration of dichloroanilines DMF solution (50 μl).

Table S1 Crystal data and structure refinement for complexes **1-4w**

Complex	**1**	**2**	**3**	**4**	**4w**
Empirical formula	$C_{21}H_{11}NO_9Zn_2$	$C_{26}H_{13}N_2O_8Zn_2$	$C_{46}H_{38}N_4O_{18}Cd_3$	$C_{383}H_{381}N_{59}O_{169}Cd_{24}$	$C_{42}H_{30}N_2O_{21}Cd_3$
Formula weight	552.05	612.12	1272	11212.07	1235.88
Temperature/K	293(2)	293(2)	293(2)	273(2)	273(2)
Wavelength/ Å	0.71073	0.71073	0.71073	0.71073	0.71073
Crystal system	Monoclinic	Monoclinic	Monoclinic	Monoclinic	Monoclinic
Space group	$P2_1/c$	P2/m	$P2_1/n$	$P2_1/n$	C2/c
a /Å	15.6058(5)	8.764(4)	14.423(3)	18.4896(6)	18.8396(12)
b/Å	13.9766(5)	15.539(7)	13.066(2)	30.3569(10)	14.5583(10)
c/Å	8.8938(3)	11.597(6)	16.263(3)	23.6755(7)	23.6467(15)
α/(°)	90	90	90	90	90
β/(°)	95.9430(10)	91.394(13)	90.933(5)	107.599(10)	107.212(2)

γ/(°)	90	90	90	90	90
Volume/ Å^3	1929.45(11)	1578.9(13)	3064.3(10)	12666.8(7)	6195.2(7)
Z	4	2	2	1	4
Calculated density/mg·m^{-3}	1.900	1.288	1.274	1.470	1.325
Absorption coefficient/mm^{-1}	2.577	1.561	1.087	1.071	1.082
F(000)	1104	614	1144	5596	2432
Crystal size/mm^3	0.26 × 0.21 × 0.15	0.20 × 0.19 × 0.10	0.32 × 0.21 × 0.12	0.42 × 0.38 × 0.35	0.22 × 0.16 × 0.11
θ range for data collection/(°)	2.915-27.559	2.948-28.794	2.951-27.744	3.04-25.50	2.957-26.00
Limiting indices	-20<=h<=20, -18<=k<=18, -11<=l<=11	-11<=h<=11, -20<=k<=20, -15<=l<=15	-18<=h<=18, -17<=k<=16, -21<=l<=21	-22<=h<=22, -36<=k<=36, -26<=l<=28	-23<=h<=23, -17<=k<=17, -29<=l<=29
Reflections collected/unique	30195 / 4456 [R(int) = 0.0413]	15144 / 3978 [R(int) = 0.1504]	44661 / 7077 [R(int) = 0.0373]	177075 / 23499 [R(int) = 0.0577]	42937 / 6086 [R(int) = 0.0393]
Data/restraints/parameters	4456 / 0 / 300	3978 / 12 / 181	7077 / 24 / 295	23499 / 663 / 1672	6086 / 18 / 309
Goodness-of-fit on F^2	1.057	1.436	1.036	1.034	1.108
R1, wR2 [I>2sigma(I)]	0.0323, 0.0823	0.1578, 0.4163	0.0252, 0.0631	0.0612, 0.1559	0.0385, 0.1051
R1, wR2 (all data)	0.0480, 0.0880	0.2642, 0.4568	0.0307, 0.0651	0.0827, 0.1672	0.0433, 0.1072
Largest diff. peak and hole / eÅ^{-3}	0.640 and -0.624	3.646 and -1.997	1.086 and -0.933	2.482 and -3.063	1.299 and -2.116
CCDC	1978663	1978664	1978665	1978666	1978667

Table S2 Selected bond lengths [Å] and angles [°] for **1**-**4w**

1	
Zn(1)-O(4)#1	1.977(2)
Zn(1)-O(1)	1.960(2)
Zn(1)-O(7)#2	1.934(2)
Zn(1)-N(1)#3	2.046(2)
Zn(2)-O(3)#4	2.015(2)
Zn(2)-O(2)	1.988(2)
Zn(2)-O(9)	1.994(2)
Zn(2)-O(5)#4	1.979(6)
Zn(2)-O(6)#4	2.104(7)
O(4)#1-Zn(1)-N(1)#3	108.72(9)
O(1)-Zn(1)-O(4)#1	101.93(9)
O(1)-Zn(1)-N(1)#3	111.60(9)
O(7)#2-Zn(1)-O(4)#1	107.27(9)

O(7)#2-Zn(1)-O(1)	127.17(10)
O(7)#2-Zn(1)-N(1)#3	99.40(9)
O(3)#4-Zn(2)-O(6)#4	101.4(3)
O(3)#4-Zn(2)-O(5)#4	96.8(3)
O(2)-Zn(2)-O(3)#4	102.27(9)
O(2)-Zn(2)-O(6)#4	92.3(2)
O(2)-Zn(2)-O(9)	94.79(9)
O(9)-Zn(2)-O(3)#4	116.84(9)
O(9)-Zn(2)-O(6)#4	152.4(2)
O(9)-Zn(2)-O(6)#4	138.1(3)
O(9)-Zn(2)-O(5)#4	97.9(2)
O(5)#4-Zn(2)-O(2)	134.5(3)
O(6)#4-Zn(2)-O(5)#4	59.3(3)
O(5)#4-Zn(2)-O(6)#4	64.4(3)

Symmetry transformations used to generate equivalent atoms: #1 -x+2, -y+1, -z+3, #2 x+1, y, z+1, #3 -x+2, y+1/2, -z+5/2, #4 -x+2, -y+1, -z+2.

2	
Zn(1)-O(3)	2.086(11)
Zn(1)-O(3)#2	2.086(11)
Zn(1)-O(4)#1	2.086(9)
Zn(1)-O(4)#3	2.086(9)
Zn(1)-N(1)#4	2.039(15)
Zn(2)-O(1)	2.036(11)
Zn(2)-O(1)#6	2.036(11)
Zn(2)-O(2)#7	2.036(10)
Zn(2)-O(2)#5	2.036(10)
Zn(2)-N(2)	2.07(2)
O(3)-Zn(1)-O(3)#2	85.4(6)
O(3)-Zn(1)-O(4)#3	89.9(4)
O(3)-Zn(1)-O(4)#1	159.2(4)
O(3)#2-Zn(1)-O(4)#1	89.9(4)
O(3)#2-Zn(1)-O(4)#3	159.2(4)
O(4)#1-Zn(1)-O(4)#3	87.3(6)
N(1)#4-Zn(1)-O(3)	95.1(5)
N(1)#4-Zn(1)-O(3)#2	95.1(5)
N(1)#4-Zn(1)-O(4)#1	105.5(5)
N(1)#4-Zn(1)-O(4)#3	105.5(5)
O(1)-Zn(2)-O(1)#6	87.9(6)
O(1)-Zn(2)-O(2)#5	161.0(6)
O(1)#6-Zn(2)-O(2)#7	161.0(6)
O(1)-Zn(2)-O(2)#7	86.0(5)
O(1)#6-Zn(2)-O(2)#5	86.0(5)
O(1)#6-Zn(2)-N(2)	102.6(6)
O(1)-Zn(2)-N(2)	102.6(6)

O(2)#7-Zn(2)-O(2)#5	93.9(6)
O(2)#7-Zn(2)-N(2)	96.3(6)
O(2)#5-Zn(2)-N(2)	96.3(6)

Symmetry transformations used to generate equivalent atoms: #1 -x+2, -y+1, -z+1; #2 x, -y+1, z; #3 -x+2, y, -z+1; #4 -x+1, -y+1, -z+1; #5 -x+2, -y, -z; #6 x, -y, z; #7 -x+2, y, -z.

3	
Cd(1)-O(3)#1	2.22(3)
Cd(1)-O(5)	2.240(7)
Cd(1)-O(7)#2	2.293(7)
Cd(1)-N(1)#3	2.313(8)
Cd(1)-O(1)	2.330(7)
Cd(1)-O(9)	2.469(9)
Cd(2)-O(8)#4	2.195(7)
Cd(2)-O(8)#2	2.195(7)
Cd(2)-O(4)#1	2.238(16)
Cd(2)-O(4)#5	2.238(16)
Cd(2)-O(9)#6	2.290(7)
Cd(2)-O(9)	2.290(7)
O(3)#1-Cd(1)-O(5)	164.9(8)
O(3)#1-Cd(1)-O(7)#2	107.1(9)
O(5)-Cd(1)-O(7)#2	85.5(3)
O(3)#1-Cd(1)-N(1)#3	88.6(7)
O(5)-Cd(1)-N(1)#3	82.5(3)
O(7)#2-Cd(1)-N(1)#3	92.2(3)
O(3)#1-Cd(1)-O(1)	78.0(9)
O(5)-Cd(1)-O(1)	89.4(3)
O(7)#2-Cd(1)-O(1)	175.0(3)
N(1)#3-Cd(1)-O(1)	87.4(3)
O(3)#1-Cd(1)-O(9)	103.4(7)
O(5)-Cd(1)-O(9)	82.4(3)
O(7)#2-Cd(1)-O(9)	98.4(3)
N(1)#3-Cd(1)-O(9)	160.8(3)
O(1)-Cd(1)-O(9)	80.6(3)
O(8)#4-Cd(2)-O(8)#2	180.0
O(8)#4-Cd(2)-O(4)#1	92.4(5)
O(8)#2-Cd(2)-O(4)#1	87.6(5)
O(8)#4-Cd(2)-O(4)#5	87.6(5)
O(8)#2-Cd(2)-O(4)#5	92.4(5)
O(4)#1-Cd(2)-O(4)#5	180.0(6)
O(8)#4-Cd(2)-O(9)#6	83.9(3)
O(8)#2-Cd(2)-O(9)#6	96.1(3)
O(4)#1-Cd(2)-O(9)#6	84.1(5)
O(4)#5-Cd(2)-O(9)#6	95.9(5)
O(8)#4-Cd(2)-O(9)	96.1(3)

O(8)#2-Cd(2)-O(9)	83.9(3)
O(4)#1-Cd(2)-O(9)	95.9(5)
O(4)#5-Cd(2)-O(9)	84.1(5)
O(9)#6-Cd(2)-O(9)	180.0

Symmetry transformations used to generate equivalent atoms: #1 -x+1/2, y-1/2, -z+1/2; #2 -x+1/2,y-1/2,-z+3/2; #3 -x, -y, -z+1; #4 x+1/2, -y+1/2, z-1/2; #5 x+1/2, -y+1/2, z+1/2; #6 -x+1, -y, -z+1.

4	
Cd(1)-N(5)	2.282(8)
Cd(1)-O(33)	2.298(5)
Cd(1)-N(2)	2.349(5)
Cd(1)-O(2)	2.351(5)
Cd(1)-O(8)	2.393(5)
Cd(1)-O(7)	2.406(5)
Cd(1)-O(1)	2.522(5)
Cd(2)-N(9)	2.291(8)
Cd(2)-O(34)	2.302(5)
Cd(2)-O(31)	2.302(5)
Cd(2)-N(12)#1	2.319(8)
Cd(2)-N(3)	2.338(5)
Cd(2)-O(16)	2.343(5)
Cd(2)-O(15)	2.534(5)
Cd(2)-O(32)	2.554(12)
Cd(3)-N(8)	2.258(7)
Cd(3)-O(36)	2.319(5)
Cd(3)-O(19)	2.331(5)
Cd(3)-O(23)	2.365(5)
Cd(3)-N(4)	2.366(5)
Cd(3)-O(24)	2.481(5)
Cd(3)-O(20)	2.512(5)
Cd(4)-O(21)	2.264(5)
Cd(4)-O(5)	2.278(5)
Cd(4)-O(37)	2.314(6)
Cd(4)-O(17)	2.407(5)
Cd(4)-O(3)	2.414(5)
Cd(4)-O(4)	2.426(5)
Cd(4)-O(18)	2.444(6)
Cd(5)-O(35)	2.277(5)
Cd(5)-O(38)	2.306(7)
Cd(5)-N(1)	2.345(5)
Cd(5)-O(12)	2.372(5)
Cd(5)-O(28)	2.394(5)
Cd(5)-O(11)	2.417(5)
Cd(5)-O(27)	2.422(5)
Cd(6)-O(10)#2	2.205(11)
Cd(6)-O(30)	2.319(5)

Cd(6)-O(13)	2.380(4)
Cd(6)-O(26)	2.398(5)
Cd(6)-O(25)	2.400(5)
Cd(6)-O(14)	2.435(5)
Cd(6)-O(29)	2.514(6)

N(5)-Cd(1)-O(33)	171.8(3)
N(5)-Cd(1)-N(2)	85.7(3)
O(33)-Cd(1)-N(2)	89.35(19)
N(5)-Cd(1)-O(2)	88.5(3)
O(33)-Cd(1)-O(2)	90.98(19)
N(2)-Cd(1)-O(2)	138.89(16)
N(5)-Cd(1)-O(8)	98.8(3)
O(33)-Cd(1)-O(8)	89.2(2)
N(2)-Cd(1)-O(8)	142.81(18)
O(2)-Cd(1)-O(8)	78.29(17)
N(5)-Cd(1)-O(7)	97.5(3)
O(33)-Cd(1)-O(7)	88.9(2)
N(2)-Cd(1)-O(7)	88.95(18)
O(2)-Cd(1)-O(7)	132.15(17)
O(8)-Cd(1)-O(7)	53.87(18)
N(5)-Cd(1)-O(1)	89.1(3)
O(33)-Cd(1)-O(1)	84.00(19)
N(2)-Cd(1)-O(1)	86.24(16)
O(2)-Cd(1)-O(1)	52.97(16)
O(8)-Cd(1)-O(1)	130.47(17)
O(7)-Cd(1)-O(1)	171.5(2)
N(9)-Cd(2)-O(34)	167.8(3)
N(9)-Cd(2)-O(31)	90.4(3)
O(34)-Cd(2)-O(31)	83.6(2)
N(9)-Cd(2)-N(12)#1	20.7(3)
O(34)-Cd(2)-N(12)#1	170.5(2)
O(31)-Cd(2)-N(12)#1	104.7(3)
N(9)-Cd(2)-N(3)	87.9(3)
O(34)-Cd(2)-N(3)	88.60(19)
O(31)-Cd(2)-N(3)	134.0(2)
N(12)#1-Cd(2)-N(3)	88.7(3)
N(9)-Cd(2)-O(16)	99.6(3)
O(34)-Cd(2)-O(16)	90.90(19)
O(31)-Cd(2)-O(16)	88.8(2)
N(12)#1-Cd(2)-O(16)	84.9(3)
N(3)-Cd(2)-O(16)	136.68(17)
N(9)-Cd(2)-O(15)	105.7(2)
O(34)-Cd(2)-O(15)	85.55(19)
O(31)-Cd(2)-O(15)	140.15(19)

N(12)#1-Cd(2)-O(15)	85.2(2)
N(3)-Cd(2)-O(15)	83.73(16)
O(16)-Cd(2)-O(15)	53.09(16)
N(9)-Cd(2)-O(32)	65.0(4)
O(34)-Cd(2)-O(32)	103.2(4)
O(31)-Cd(2)-O(32)	51.2(3)
N(12)#1-Cd(2)-O(32)	85.8(4)
N(3)-Cd(2)-O(32)	87.4(3)
O(16)-Cd(2)-O(32)	134.5(3)
O(15)-Cd(2)-O(32)	167.4(3)
N(8)-Cd(3)-O(36)	171.6(3)
N(8)-Cd(3)-O(19)	96.3(3)
O(36)-Cd(3)-O(19)	90.43(19)
N(8)-Cd(3)-O(23)	88.5(3)
O(36)-Cd(3)-O(23)	83.3(2)
O(19)-Cd(3)-O(23)	133.00(19)
N(8)-Cd(3)-N(4)	88.1(3)
O(36)-Cd(3)-N(4)	90.25(19)
O(19)-Cd(3)-N(4)	137.72(17)
O(23)-Cd(3)-N(4)	89.02(19)
N(8)-Cd(3)-O(24)	90.2(3)
O(36)-Cd(3)-O(24)	86.1(2)
O(19)-Cd(3)-O(24)	79.75(17)
O(23)-Cd(3)-O(24)	53.41(19)
N(4)-Cd(3)-O(24)	142.43(18)
N(8)-Cd(3)-O(20)	97.8(3)
O(36)-Cd(3)-O(20)	90.18(19)
O(19)-Cd(3)-O(20)	53.52(16)
O(23)-Cd(3)-O(20)	170.6(2)
N(4)-Cd(3)-O(20)	84.20(16)
O(24)-Cd(3)-O(20)	133.11(17)
N(8)-Cd(3)-C(49)	97.8(3)
O(36)-Cd(3)-C(49)	90.4(2)
O(19)-Cd(3)-C(49)	26.70(17)
O(23)-Cd(3)-C(49)	159.1(2)
N(4)-Cd(3)-C(49)	111.02(18)
O(24)-Cd(3)-C(49)	106.38(19)
O(20)-Cd(3)-C(49)	26.83(17)
O(21)-Cd(4)-O(5)	169.4(2)
O(21)-Cd(4)-O(37)	105.5(2)
O(5)-Cd(4)-O(37)	85.0(2)
O(21)-Cd(4)-O(17)	90.57(19)
O(5)-Cd(4)-O(17)	88.9(2)
O(37)-Cd(4)-O(17)	90.6(2)
O(21)-Cd(4)-O(3)	94.25(19)

O(5)-Cd(4)-O(3)	87.6(2)
O(37)-Cd(4)-O(3)	81.7(2)
O(17)-Cd(4)-O(3)	171.8(2)
O(21)-Cd(4)-O(4)	86.8(2)
O(5)-Cd(4)-O(4)	85.9(2)
O(37)-Cd(4)-O(4)	134.5(2)
O(17)-Cd(4)-O(4)	133.69(18)
O(3)-Cd(4)-O(4)	53.43(18)
O(21)-Cd(4)-O(18)	83.0(2)
O(5)-Cd(4)-O(18)	88.2(2)
O(37)-Cd(4)-O(18)	143.0(2)
O(17)-Cd(4)-O(18)	52.86(18)
O(3)-Cd(4)-O(18)	134.39(18)
O(4)-Cd(4)-O(18)	80.97(18)
O(35)-Cd(5)-O(38)	177.7(3)
O(35)-Cd(5)-N(1)	92.5(2)
O(38)-Cd(5)-N(1)	89.2(3)
O(35)-Cd(5)-O(12)	85.8(2)
O(38)-Cd(5)-O(12)	91.9(3)
N(1)-Cd(5)-O(12)	139.70(18)
O(35)-Cd(5)-O(28)	93.2(2)
O(38)-Cd(5)-O(28)	86.6(3)
N(1)-Cd(5)-O(28)	137.33(17)
O(12)-Cd(5)-O(28)	82.91(17)
O(35)-Cd(5)-O(11)	92.5(2)
O(38)-Cd(5)-O(11)	86.0(3)
N(1)-Cd(5)-O(11)	85.94(18)
O(12)-Cd(5)-O(11)	54.00(18)
O(28)-Cd(5)-O(11)	135.91(18)
O(35)-Cd(5)-O(27)	91.98(19)
O(38)-Cd(5)-O(27)	89.8(3)
N(1)-Cd(5)-O(27)	83.84(17)
O(12)-Cd(5)-O(27)	136.43(17)
O(28)-Cd(5)-O(27)	53.73(16)
O(11)-Cd(5)-O(27)	169.00(18)
O(10)#2-Cd(6)-O(13)	93.3(3)
O(30)-Cd(6)-O(13)	88.37(19)
O(10)#2-Cd(6)-O(26)	93.7(3)
O(30)-Cd(6)-O(26)	82.1(2)
O(13)-Cd(6)-O(26)	142.73(17)
O(10)#2-Cd(6)-O(25)	88.4(4)
O(30)-Cd(6)-O(25)	91.44(19)
O(13)-Cd(6)-O(25)	163.09(18)
O(26)-Cd(6)-O(25)	53.72(17)
O(10)#2-Cd(6)-O(14)	92.2(4)

O(30)-Cd(6)-O(14)	84.9(2)
O(13)-Cd(6)-O(14)	54.19(16)
O(26)-Cd(6)-O(14)	88.98(17)
O(25)-Cd(6)-O(14)	142.62(17)
O(10)#2-Cd(6)-O(29)	131.6(4)
O(30)-Cd(6)-O(29)	53.2(2)
O(13)-Cd(6)-O(29)	88.81(18)
O(26)-Cd(6)-O(29)	112.88(19)
O(25)-Cd(6)-O(29)	77.63(18)
O(14)-Cd(6)-O(29)	126.23(19)

Symmetry transformations used to generate equivalent atoms: #1 -x+2, -y+2, -z+1; #2 x-1/2, -y+3/2, z-1/2.

4w	
Cd(1)-O(9)	2.251(5)
Cd(1)-O(3)	2.296(3)
Cd(1)-O(3)#1	2.296(3)
Cd(1)-O(8)	2.387(3)
Cd(1)-O(8)#1	2.387(3)
Cd(1)-O(7)	2.457(3)
Cd(1)-O(7)#1	2.457(3)
Cd(2)-O(10)	2.298(3)
Cd(2)-N(1)#2	2.335(3)
Cd(2)-O(6)	2.362(3)
Cd(2)-O(1)	2.364(3)
Cd(2)-O(11)	2.367(4)
Cd(2)-O(2)	2.438(3)
Cd(2)-O(5)	2.457(3)
Cd(2)-C(1)	2.749(4)
Cd(2)-C(9)	2.751(3)
O(9)-Cd(1)-O(3)	94.49(9)
O(9)-Cd(1)-O(3)#1	94.49(9)
O(3)-Cd(1)-O(3)#1	171.01(18)
O(9)-Cd(1)-O(8)	137.29(7)
O(3)-Cd(1)-O(8)	85.92(12)
O(3)#1-Cd(1)-O(8)	87.48(11)
O(9)-Cd(1)-O(8)#1	137.29(7)
O(3)-Cd(1)-O(8)#1	87.48(11)
O(3)#1-Cd(1)-O(8)#1	85.92(12)
O(8)-Cd(1)-O(8)#1	85.42(14)
O(9)-Cd(1)-O(7)	84.74(8)
O(3)-Cd(1)-O(7)	89.59(10)
O(3)#1-Cd(1)-O(7)	91.23(10)
O(8)-Cd(1)-O(7)	52.56(10)
O(8)#1-Cd(1)-O(7)	137.97(11)

O(9)-Cd(1)-O(7)#1	84.74(8)
O(3)-Cd(1)-O(7)#1	91.23(10)
O(3)#1-Cd(1)-O(7)#1	89.59(10)
O(8)-Cd(1)-O(7)#1	137.97(11)
O(8)#1-Cd(1)-O(7)#1	52.56(10)
O(7)-Cd(1)-O(7)#1	169.47(16)
O(10)-Cd(2)-N(1)#2	91.45(13)
O(10)-Cd(2)-O(6)	92.72(12)
N(1)#2-Cd(2)-O(6)	137.47(9)
O(10)-Cd(2)-O(1)	83.60(12)
N(1)#2-Cd(2)-O(1)	139.12(10)
O(6)-Cd(2)-O(1)	83.38(10)
O(10)-Cd(2)-O(11)	175.14(12)
N(1)#2-Cd(2)-O(11)	91.83(14)
O(6)-Cd(2)-O(11)	82.44(13)
O(1)-Cd(2)-O(11)	96.24(14)
O(10)-Cd(2)-O(2)	95.86(14)
N(1)#2-Cd(2)-O(2)	86.89(10)
O(6)-Cd(2)-O(2)	134.56(11)
O(1)-Cd(2)-O(2)	53.61(10)
O(11)-Cd(2)-O(2)	87.91(16)
O(10)-Cd(2)-O(5)	88.87(11)
N(1)#2-Cd(2)-O(5)	84.08(9)
O(6)-Cd(2)-O(5)	53.74(9)
O(1)-Cd(2)-O(5)	136.07(10)
O(11)-Cd(2)-O(5)	87.89(13)
O(2)-Cd(2)-O(5)	169.91(10)

Symmetry transformations used to generate equivalent atoms: #1 -x+1, y, -z+1/2; #2 x, -y+2, z+1/2.

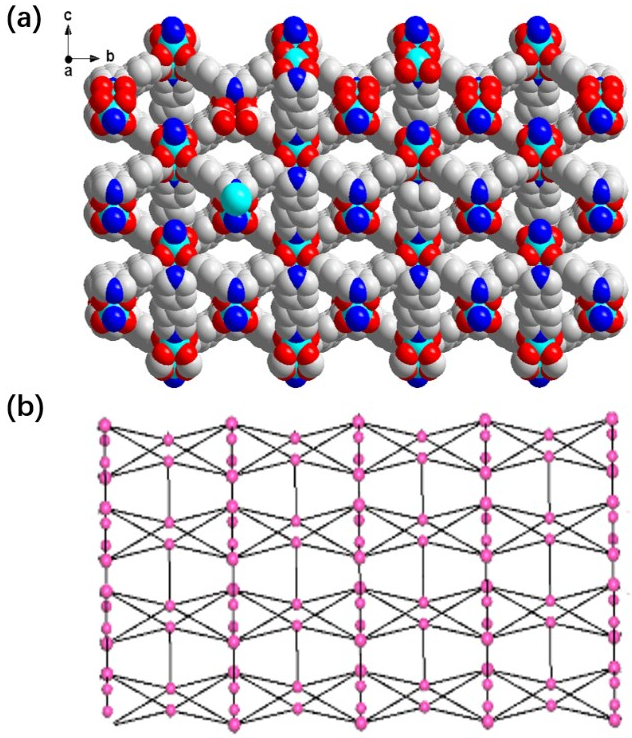

Fig. S1 Spatial filling diagram (a) and 3D topological net (b) of complex **2** with a point symbol of $\{4^2.\ 6\}\{4^6.\ 6^4\}\{4^8.\ 6.\ 7^4.\ 8^8\}$.

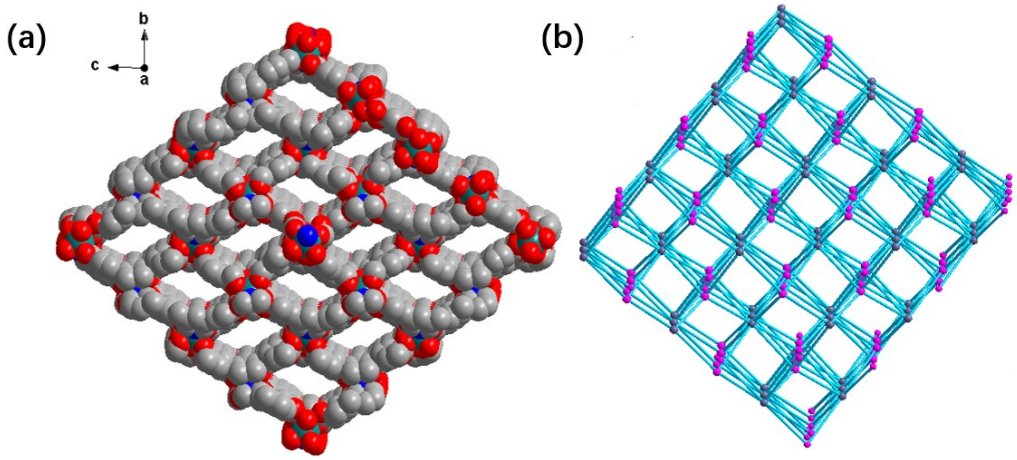

Fig. S2 Spatial filling diagram (a) and 3D topological net (b) of complex **3** with a point symbol of $\{4^{12}.\ 6^{12}.\ 8^4\}\ \{4^6\}_2$.

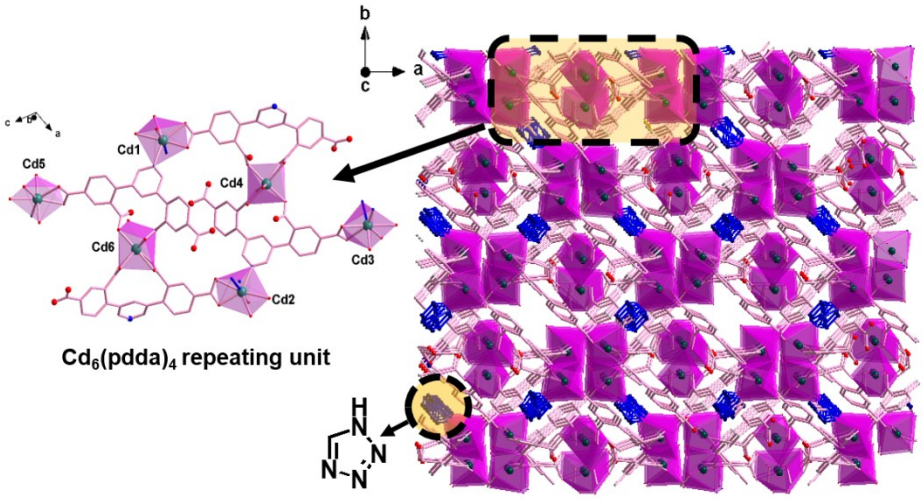

Fig. S3 Hexa-nuclear $Cd_6(pdda)_4$ repeating units and 3D structure of complex **4**.

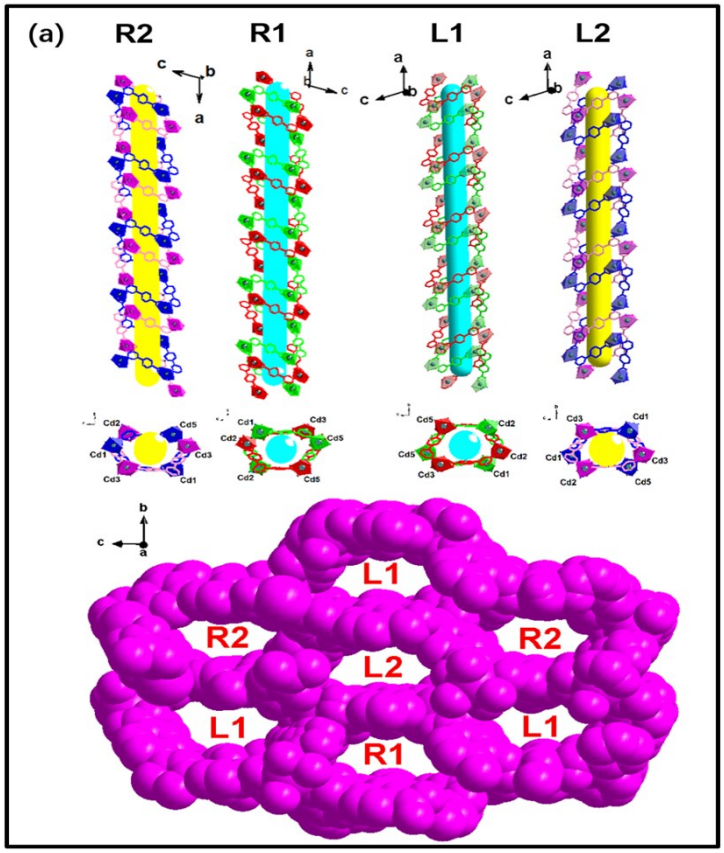

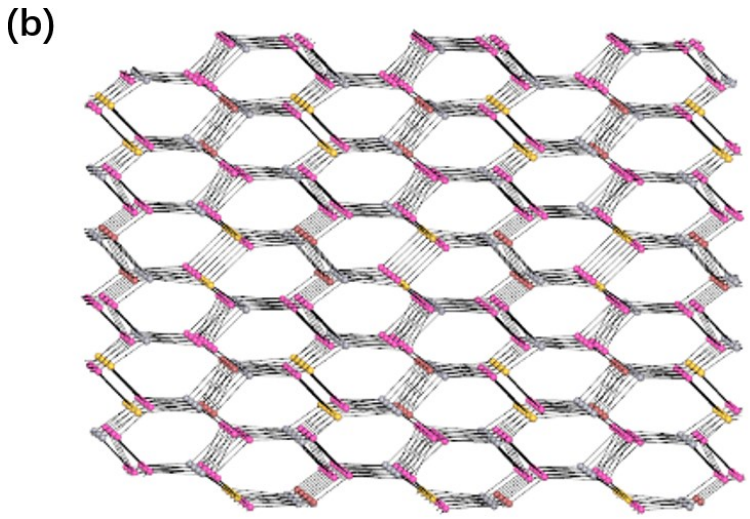

Fig. S4 (a) Two kinds of chiral helixes (L1/R1 and L2/R2) and space-filling representation of complex **4** with the arrangement of chiral nanotube channel. (b) 3D topological net of complex **4** with a point symbol of $\{4.\ 6^2.\ 8^3\}\ \{4.\ 6^3.\ 8.\ 10\}\{4^2.\ 6^3.\ 8\}_5\ \{6^2.\ 8\}$.

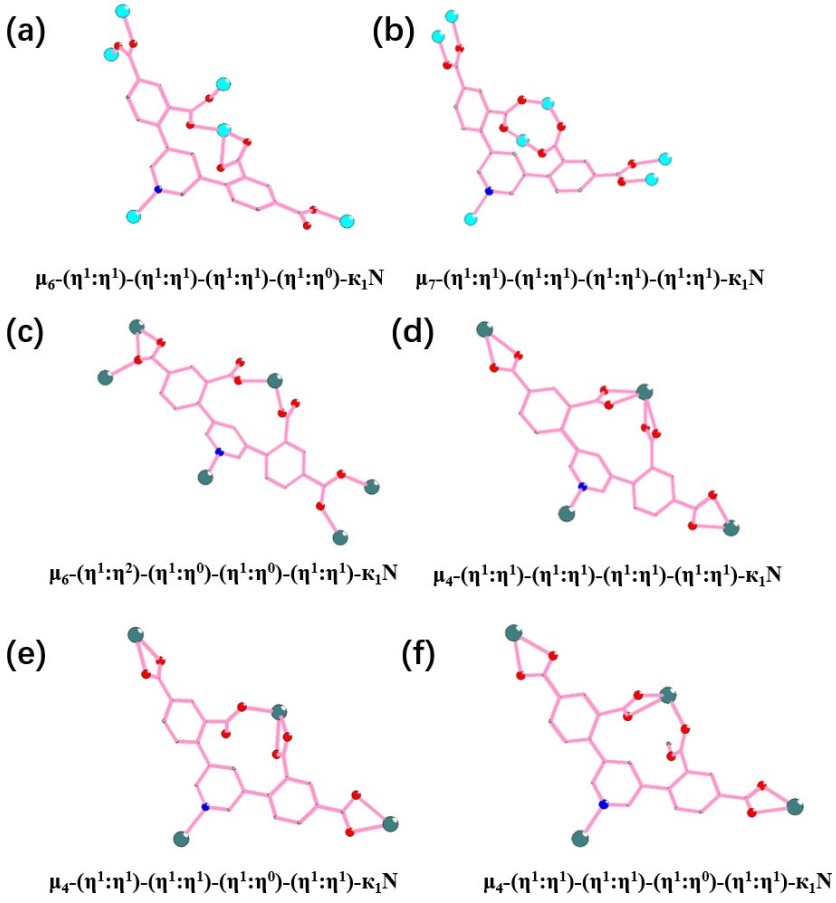

Scheme S1 Coordination modes of H_4pdda for **1** (a), **2** (b), **3** (c), **4** (d) and (e), **4w** (f).

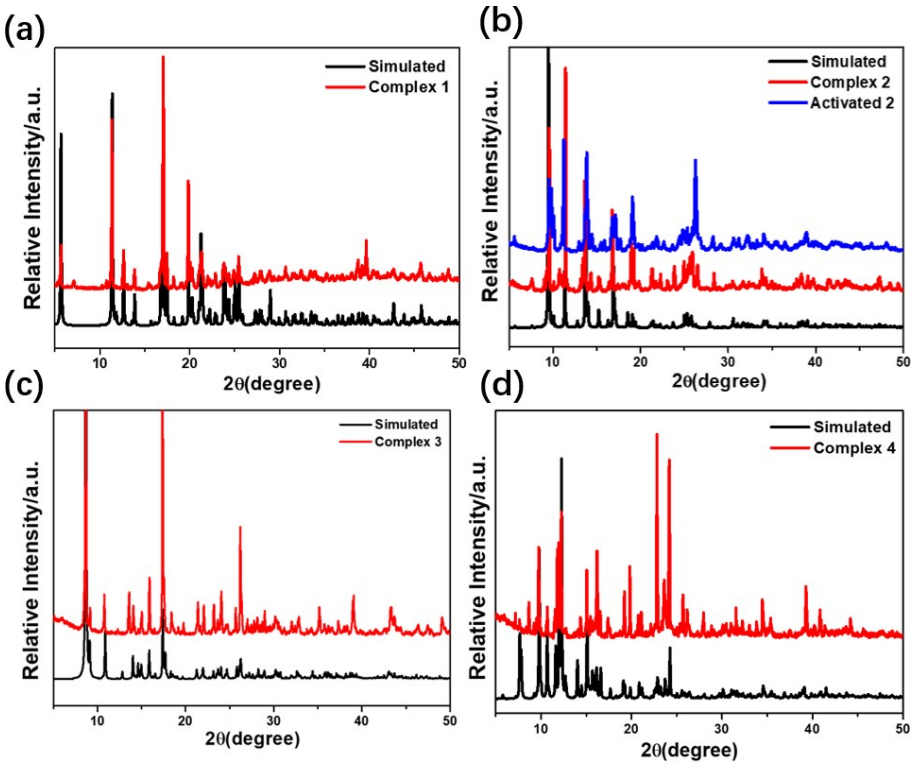

Fig. S5 PXRD patterns of complexes **1**-**4**

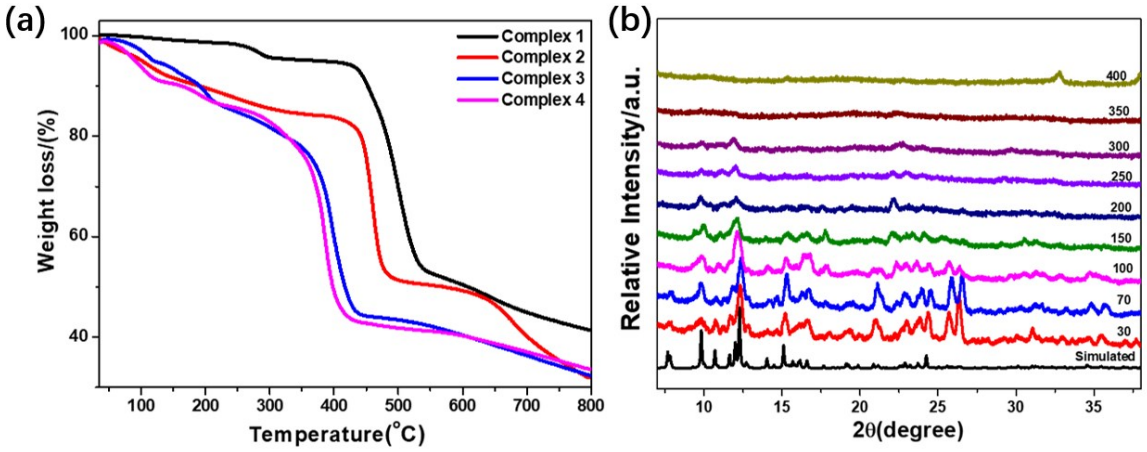

Fig. S6 The TGA curves of complexes **1**-**4**. (a) The variable temperature PXRD results of complex **4**. (b)

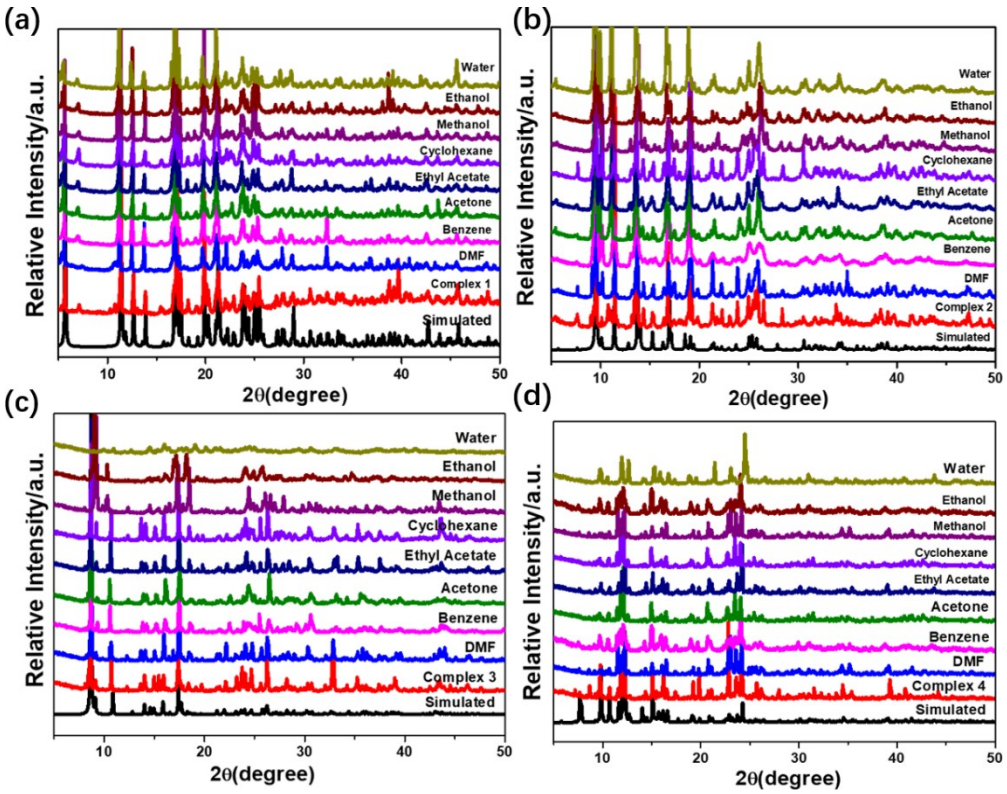

Fig. S7 PXRD patterns (a)-(d) of **1-4** after being immersed in common solvents.

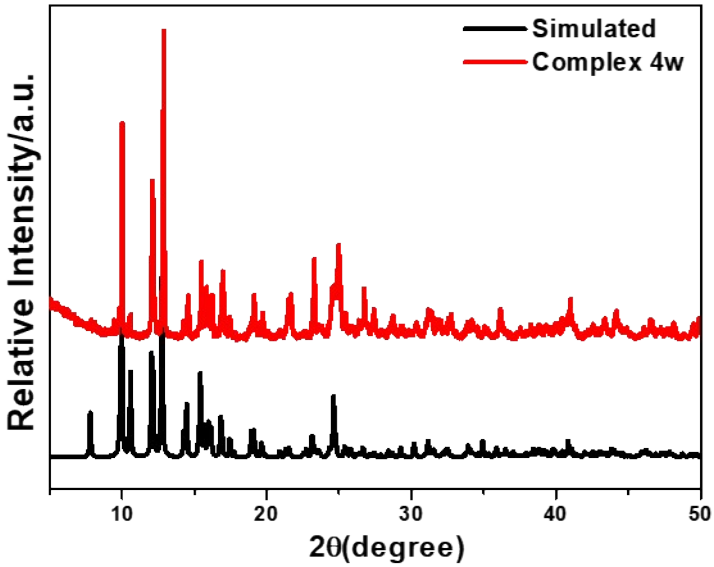

Fig. S8 PXRD pattern of complex **4w**

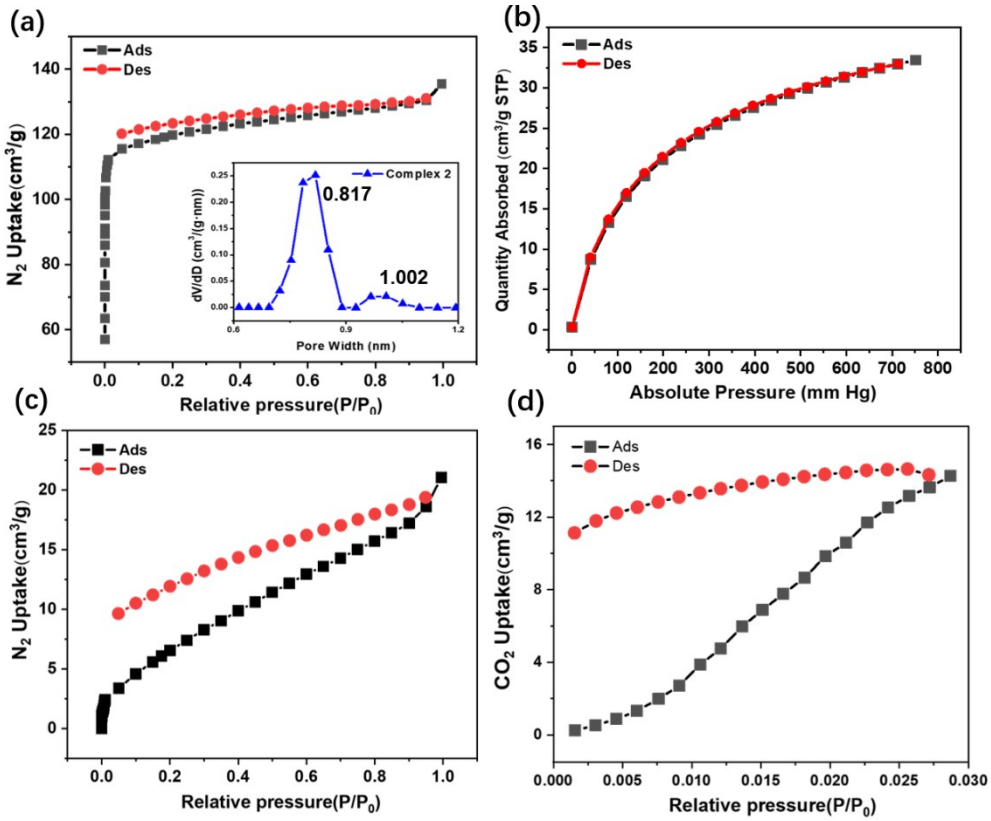

Fig. S9 (a, c) N_2 sorption isotherms at 77 K and pore size distributions of activated **2** and **4**; (b, d) CO_2 sorption isotherms of activated **2** and **4** at 273 K.

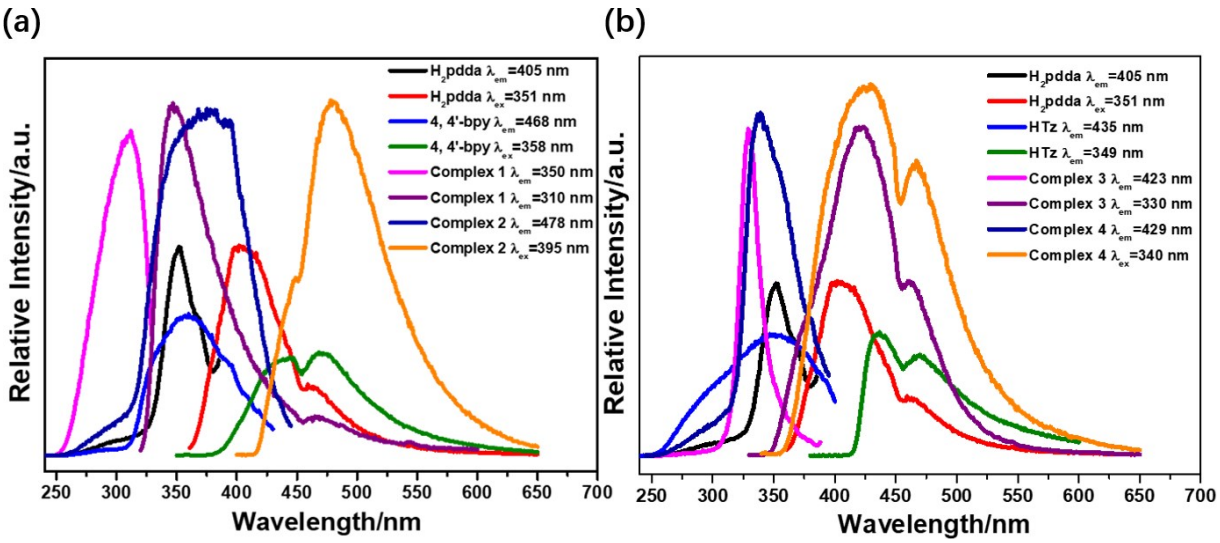

Fig. S10 Solid excitation and emission spectra of **1-4** and the free ligands.

Optimization and verification of sensing experiments: Specifically, there are two experimental steps involving optimization experiments. Firstly, for the preparation of Ln(III)@**4** hybrid system by Ln(III)-ion exchange, the ion-exchange solvent that we initially selected was volatile methanol based on the results of solvent/chemical stability, because methanol could not only contribute to the rapid preparation of the dry hybrid, but can replace the guest DMF in the structure **4** for increasing the porosity of Ln(III)@**4** and enhancing the sensing sensitivity. However, the results show that **4** changes to **4w** after the exchange process completed and the Ln(III)@**4** hybrid can't be obtained. Therefore, we selected DMF as the exchange solvent, because it was used as the synthetic solvent of complex **4**, in which **4** will be more stable and thereby successfully preparing the Ln(III)@**4** hybrid system, as shown by the relevant PXRD test results. (Fig. S1a) Next, we need to consider Ln(III) concentration in DMF for subsequent ion-exchange experiment, which will directly affect the structure integrity of **4** and the luminescent properties of Ln(III)@**4**. We selected a higher Ln(III) concentration of 10^{-1} M for the functionalization experiment of Ln(III)-ion exchange based on previous experimental experience in order to get fully exchanged products. The newly as-synthesized **4** sample (100 mg) was immersed in DMF stirred for two days with the Ln(III) concentration of 10^{-1} M, then filtered, washed and dried to obtain 10^{-1} M Ln(III)@**4** hybrids, and the fluorescence studies show the excellent sensitization of **4** to Tb(III) ions. Furthermore, 10^{-2} M and 10^{-3} M Ln(III)@**4** hybrids were fabricated with the same method. PXRD results show that compared to 10^{-1} M Tb(III)@**4** the intensities of the diffraction peaks of 10^{-2} M and 10^{-3} M Ln(III)@**4** are more obvious and match better with simulated **4**, which prove that the structure of **4** can maintain high integrity during the exchange process at lower Tb(III) concentration (Fig. S1b), and solid-state fluorescence test results show that as the Tb(III) concentration increases in DMF, the characteristic fluorescence emissions of the resulting-hybrids increase gradually. (Fig. S1c) Based on these, 10^{-2} M Tb(III)@**4** hybrid can be regarded as an optimal option, which shows better structural integrity and luminescence properties for subsequent sensing experiments. In addition, in the luminescence sensing experiment, the amount of Tb(III)@**4** is 3 mg in 3 ml test solution, which is based on the previous experience of sensing work, that is, generally the amount of samples in the range of 2-3 mg in the 3 ml solution system will not affect the final sensing results.

The second optimization step is about Tb(III)@**4** as a sensor for sensing biomarker dichloroaniline in DMF reconstructed urine samples for judging actual sensing potential. In this process, the ratio of urine sample to DMF need to be considered, because the complex **4** will rapidly change from **4** to **4w** in pure aqueous solution and should destroy the ion-exchange system Tb(III)@**4**, thus Tb(III)@**4** cannot be used in pure urine systems for sensing dichloroaniline. But we believe that it is feasible to perform sensing in urine systems reconstructed by DMF, which is inspired by similar sensing work published by *Zhang et al*.[1] They had done the sensing of LPA as a cancer biomarker, and the sensing environment is lyophilized plasma reconstituted by MeOH. The simple experimental tests show that the optimal ratio of urine sample to DMF should be 1 to 10, under which Tb(III)@**4** can stably exist as PXRD results (Fig. S15). As DMF proportion decreases, we readily find that the luminescence emission of Tb(III)@**4** quenched obviously, which may due to the generation of the neutral framework of **4w** destroying the integrity of the Tb(III)@**4**, and the quenching effect of OH-oscillators form water molecules.

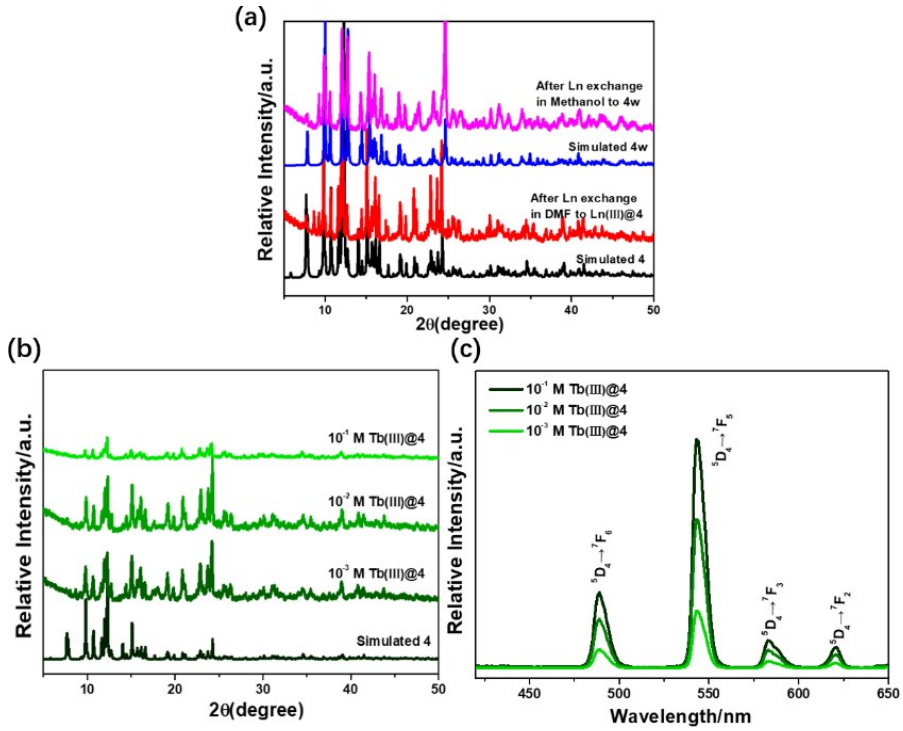

Fig. S11 (a) PXRD patterns of complex **4** after Ln(III) exchange in methanol and DMF. (b) PXRD patterns of 10^{-1}, 10^{-2} and 10^{-3} M Tb(III)@**4** hybrids. (c) The Solid-state emission spectra of 10^{-1}, 10^{-2} and 10^{-3} M Tb(III)@**4** hybrids under the excitation wavelength of 300 nm.

[1] S. Y. Zhang, Wei Shi, P. Cheng, M. J. Zaworotko. *J. Am. Chem. Soc.* 2015, 137, 12203.

Table S3 The ICP-MS results and the calculated molar ratios of tested compounds.

Compound	Cd (ppm)	Tb (ppm)	Eu (ppm)	Sm (ppm)	Dy (ppm)	Molar Ratio
10^{-2} M Tb(III)@**4**	81.67	7.32				Cd/Tb 15.7/1
10^{-2} M Eu(III)@**4**	82.28		7.68			Cd/Eu 14.4/1
10^{-2} M Sm(III)@**4**	81.86			7.13		Cd/Sm 15.4/1
10^{-2} M Dy(III)@**4**	82.06				7.08	Cd/Dy 16.6/1

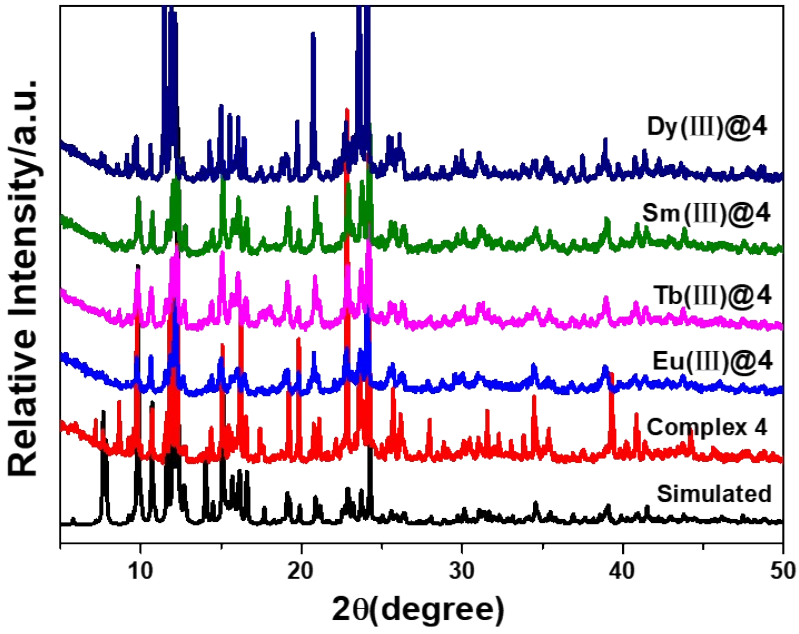

Fig. S12 PXRD patterns of complex **4** and Ln(III)@**4** (Ln(III) = Eu(III), Tb(III), Sm(III), Dy(III)).

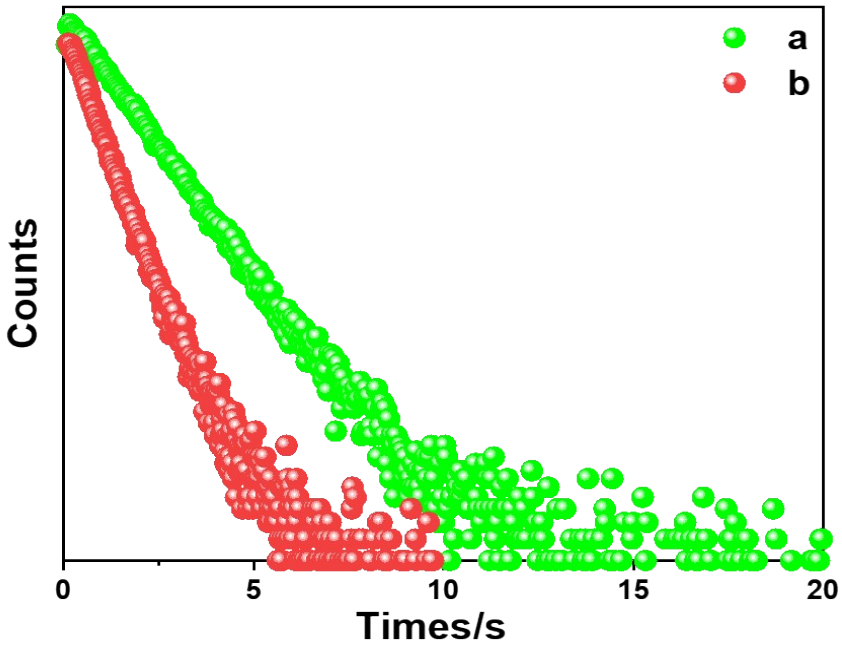

Fig. S13 Emission decay profiles of $^5D_4$ Tb(III) in Tb(III)@**4** (a), and $^5D_0$ Eu(III) in Eu(III)@**4** (b).

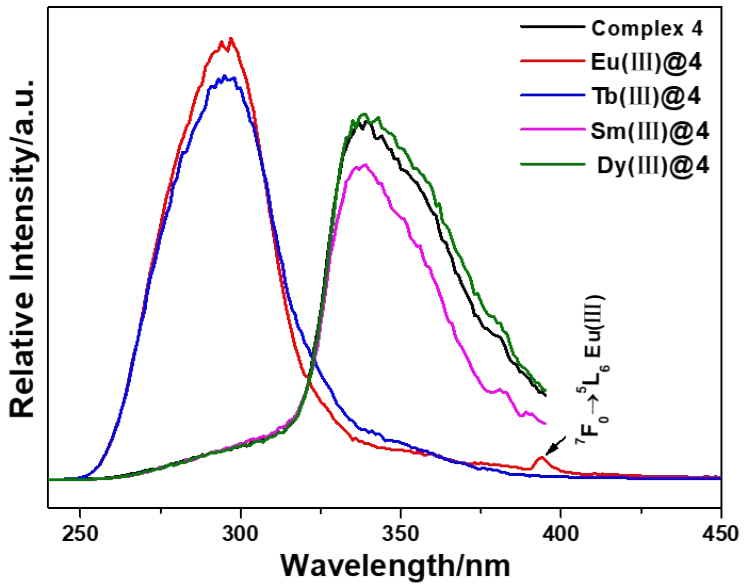

Fig. S14 Solid excitation spectra of Ln(III)@**4**.

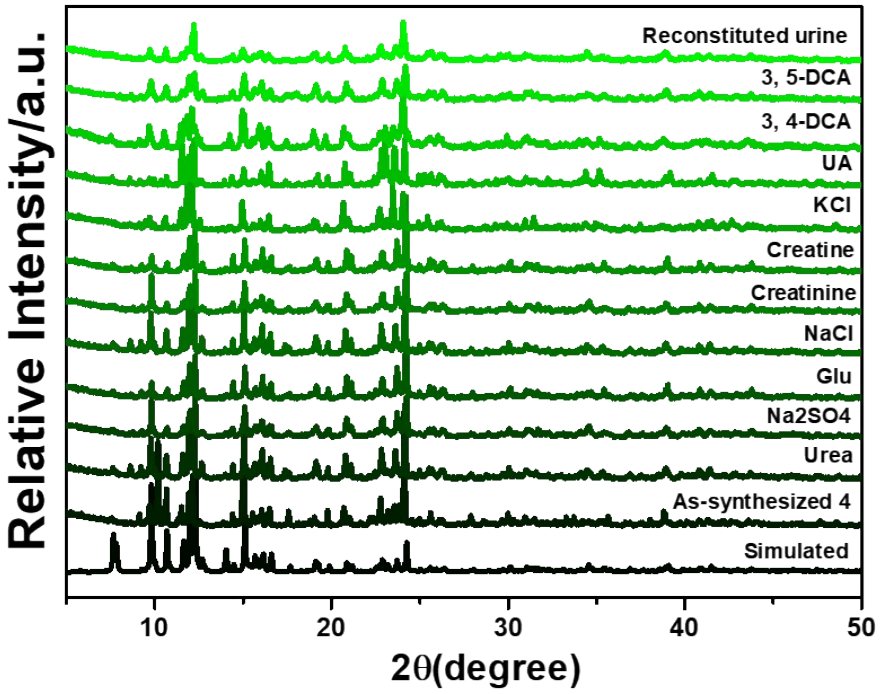

Fig. S15 PXRD patterns of as-synthesized and simulated **4**, and Tb(III)@**4** immersing in different solutions of urine chemicals and reconstituted urine sample.

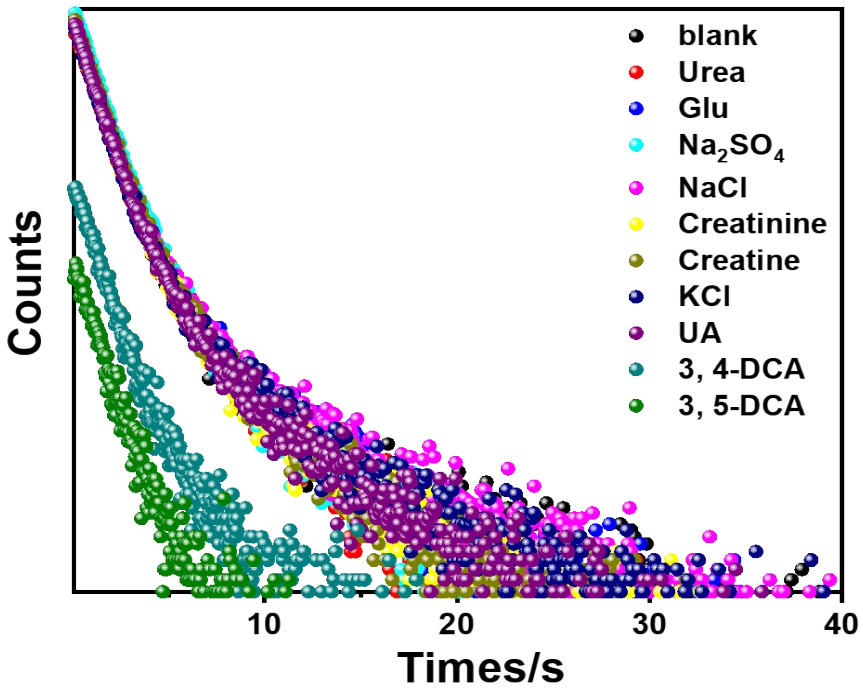

Fig. S16 Emission decay profiles of $^5D_4$ Tb(III) in Tb(III)@**4** towards various urine chemicals in DMF.

Table S4 Responses of luminescence lifetimes of Tb(III)@**4** towards various urine chemicals in DMF solutions (λ_{ex} = 300 nm and λ_{em} = 544 nm).

Materials	τ (μs)
DMF	2532.47
NaCl	2702.90
KCl	2633.26
Na_2SO_4	2231.69
Glu	2460.19
Urea	2362.23
UA	2386.96
Creatine	2345.02
Creatinine	2298.89
3, 4-DCA	1951.53
3, 5-DCA	1839.04

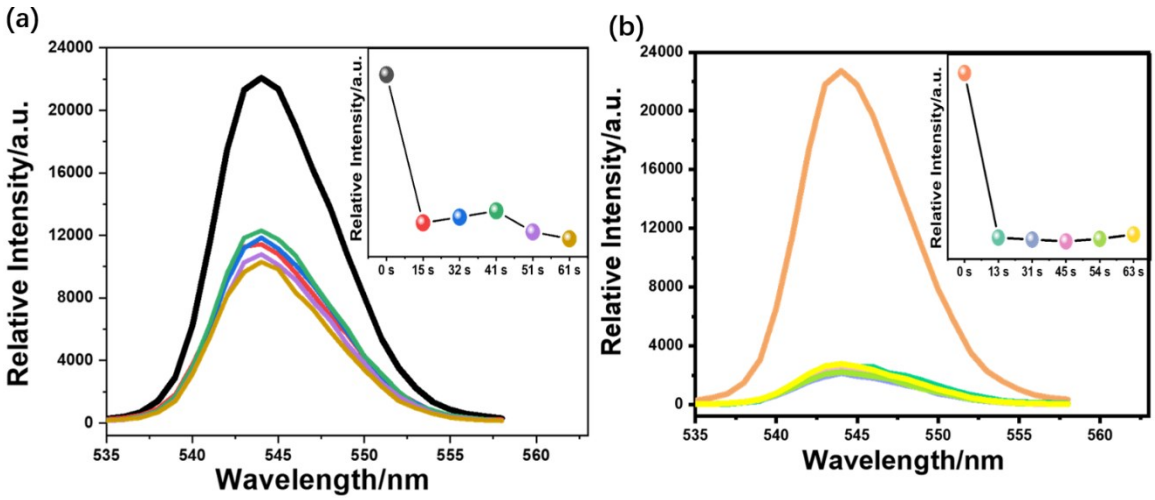

Fig. S17 Time dependence of emission spectra and intensities at 544 nm (excited at 300 nm) of Tb(III)@**4** suspension upon addition of 3, 4-DCA (a) and 3, 5-DCA (b).

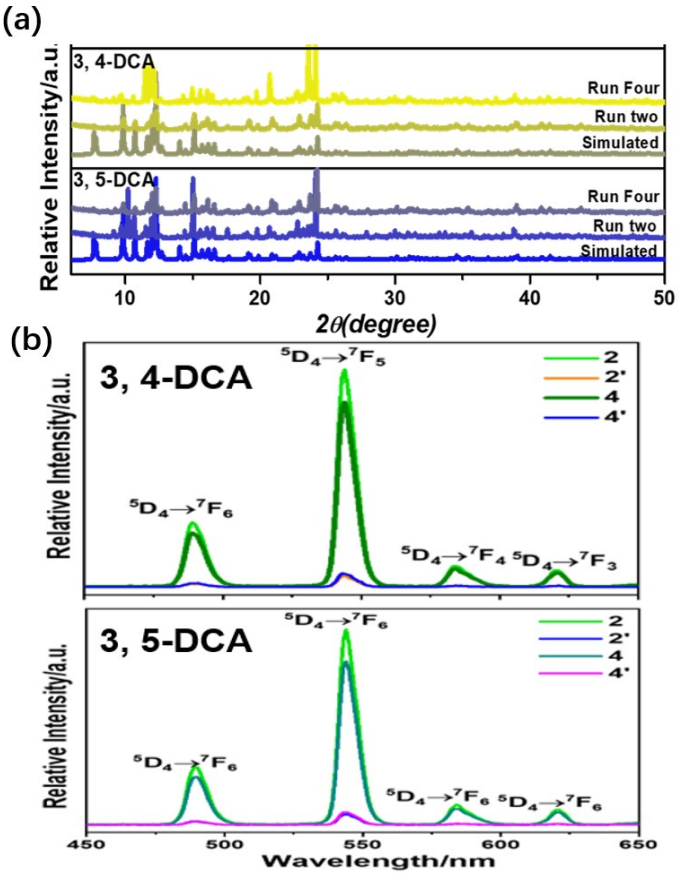

Fig. S18 PXRD patterns of Tb(III)@**4** after two and four recycles of sensing for 3, 4-DCA and 3, 5-DCA in DMF (a), and Emission spectra of Tb(III)@**4** upon four recycles of sensing for 3, 4-DCA and 3, 5-DCA in DMF. (b)

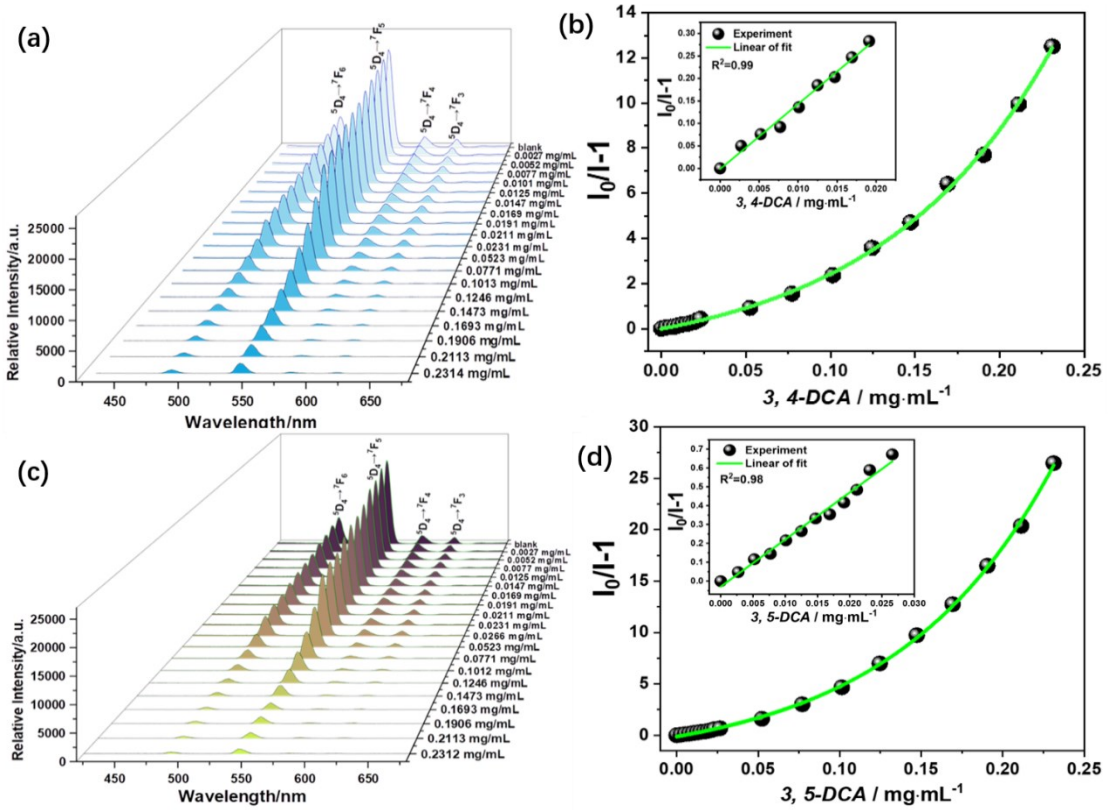

Fig. S19 Emission spectra of Tb(III)@**4** dispersed in reconstituted urine samples with different concentrations of 3, 4-DCA (a) and 3, 5-DCA (c). S-V curve of I_0/I-1 versus concentration of 3, 4-DCA (b) and 3, 5-DCA (d).

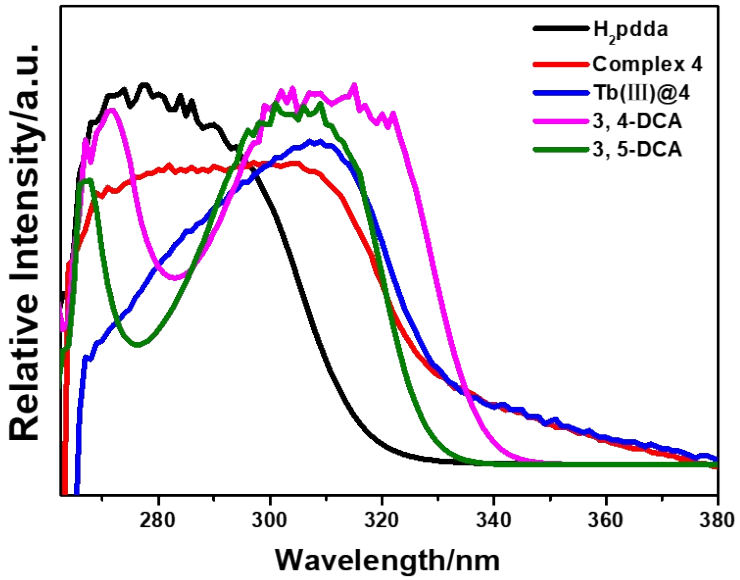

Fig. S20 UV-Vis absorption spectra of H_2pdda, complex **4**, Tb(III)@**4** and 3, 4-DCA and 3, 5-DCA in DMF.

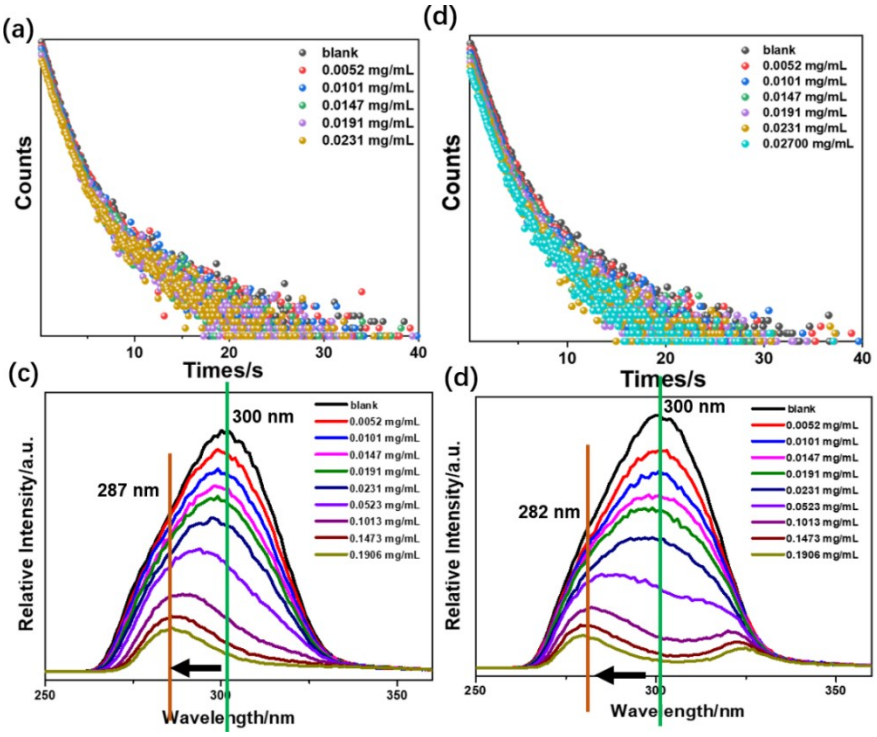

Fig. S21 Emission decay profiles of $^5D_4$ Tb(III) in Tb(III)@**4**/DMF suspensions under low concentrations of 3, 4-DCA (a) and 3, 5-DCA (b). Excitation spectra of Tb(III)@**4**/DMF suspensions under different concentrations of 3, 4-DCA (c) and 3, 5-DCA (d).

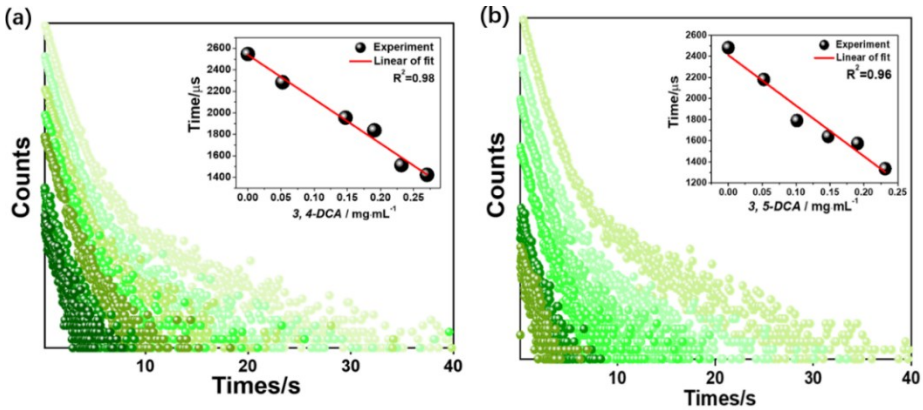

Fig. S22 Emission decay profiles of $^5D_4$ Tb(III) in Tb(III)@**4**/DMF suspensions under different concentrations of 3, 4-DCA (a) and 3, 5-DCA (b) and linear relationships between lifetime values and concentrations of dichloroanilines (above 0.0523 mg mL^{-1}).